

Supporting Information

for *Adv. Sci.*, DOI: 10.1002/advs.202103248

SARS-CoV-2 N protein induces acute kidney injury via
Smad3-dependent G1 cell cycle arrest mechanism

Wenbiao Wang^{1,2,4,6,#}, *Junzhe Chen*^{1,3,#}, *Dingwen Hu*⁵, *Pan Pan*²,
*Liyang Liang*¹, *Wenjing Wu*^{1,4}, *Ying Tang*³, *Xiao R Huang*^{1,4},
Xueqing Yu^{4,**}, *Jianguo Wu*^{2,5,**}, *Hui Y Lan*^{1,6,*}

Supplementary Information

SARS-CoV-2 N protein induces acute kidney injury via Smad3-dependent G1 cell cycle arrest mechanism

Wenbiao Wang^{1,2,4,6,#}, Junzhe Chen^{1,3,#}, Dingwen Hu⁵, Pan Pan², Liying Liang¹, Wenjing Wu^{1,4}, Ying Tang³, Xiao R. Huang^{1,4}, Xueqing Yu^{4,**}, Jianguo Wu^{2,5,**}, Hui Y. Lan^{1,6*}.

¹ Departments of Medicine & Therapeutics, Li Ka Shing Institute of Health Sciences, and Lui Che Woo Institute of Innovative Medicine, The Chinese University of Hong Kong, Hong Kong, China.

² Guangdong Provincial Key Laboratory of Virology, Institute of Medical Microbiology, Jinan University, Guangzhou 510632, China.

³ Department of Nephrology, The Third Affiliated hospital, Southern Medical University, Guangzhou, China.

⁴ Guangdong-Hong Kong Joint Laboratory for Immunological and Genetic Kidney Disease, Guangdong Academy of Medical Science, Guangdong Provincial People's Hospital, Guangzhou, China.

⁵ State Key Laboratory of Virology, College of Life Sciences, Wuhan University, Wuhan 430072, China.

⁶ The Chinese University of Hong Kong-Guangdong Academy of Sciences/Guangdong Provincial People's Hospital Joint Research Laboratory on Immunological and Genetic Kidney Diseases, The Chinese University of Hong Kong, Hong Kong, China.

#Wenbiao Wang, Junzhe Chen contributed equally to this study

***Correspondence:** Hui-Yao Lan, Departments of Medicine & Therapeutics, Li Ka Shing Institute of Health Sciences, The Chinese University of Hong Kong, Hong Kong, China. E-mail: hylan@cuhk.edu.hk.

****Co-correspondence:** Jianguo Wu, jwu898@jnu.edu.cn; Xueqing Yu, yuxq@mail.sysu.edu.cn

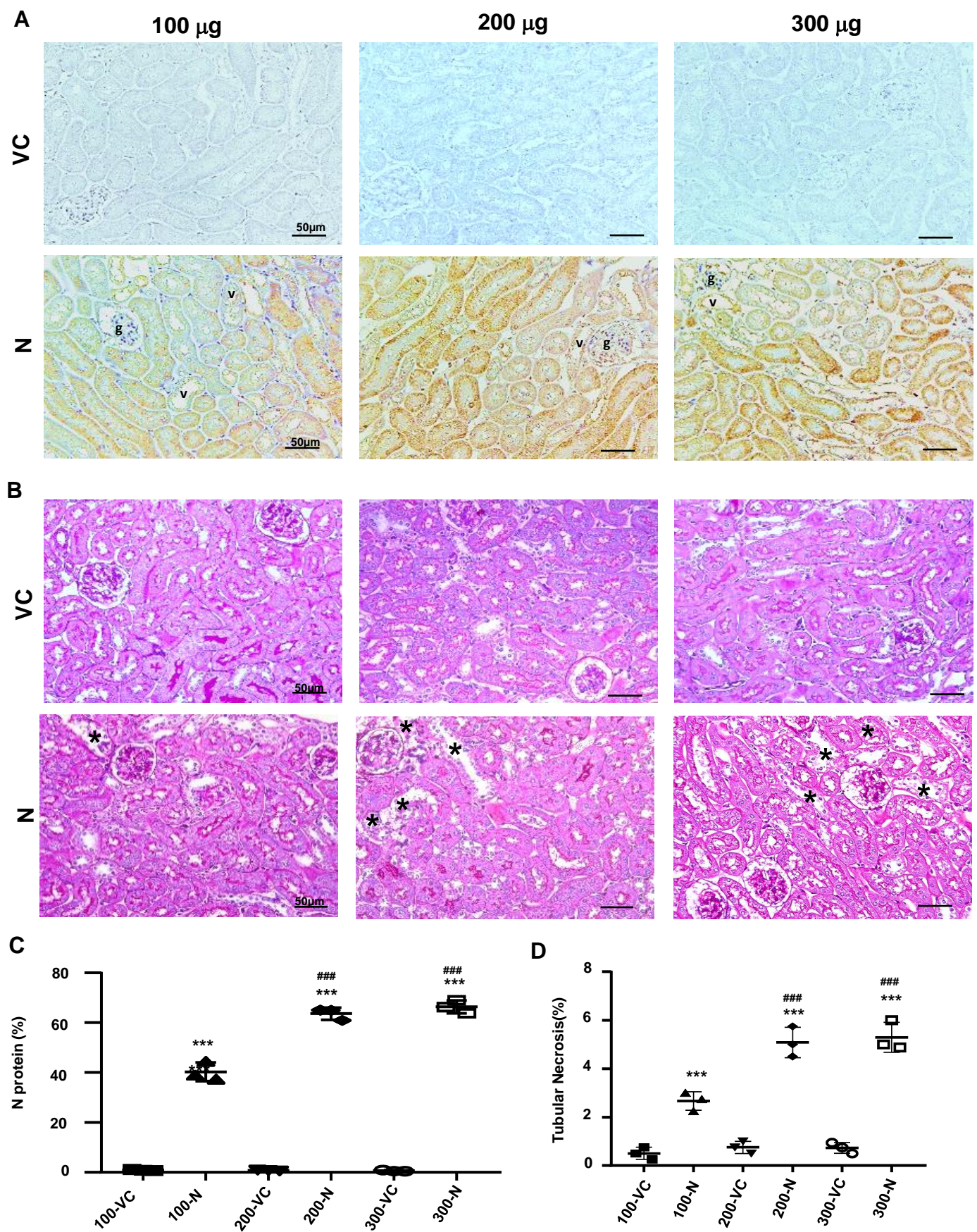


Figure S1. Ultrasound-microbubble-mediated kidney-specific SARS-CoV-2 N protein (N) expression induces tubular necrosis in a dose-dependent manner. (A) N protein immunostaining; (B) PAS-staining; (C) Semi-quantitative analysis of N protein; (D) Semi-quantitative analysis of tubular necrosis (*). Note that SARS-CoV-2 N protein plasmid transfer results in overexpression of N protein and tubular necrosis in a dose-dependent manner, peaking at 200 $\mu\text{g}/\text{mouse}$. Each dot represents one mouse and data are expressed as the mean \pm SEM for groups of 3 mice. * $p < 0.001$ versus vector control (VC); #### $p < 0.001$ versus SARS-CoV-2 N-expressing plasmid at 100 $\mu\text{g}/\text{mouse}$ (100-N). g, glomerulus; v, vascular cells. Scale bar=50 μm .**

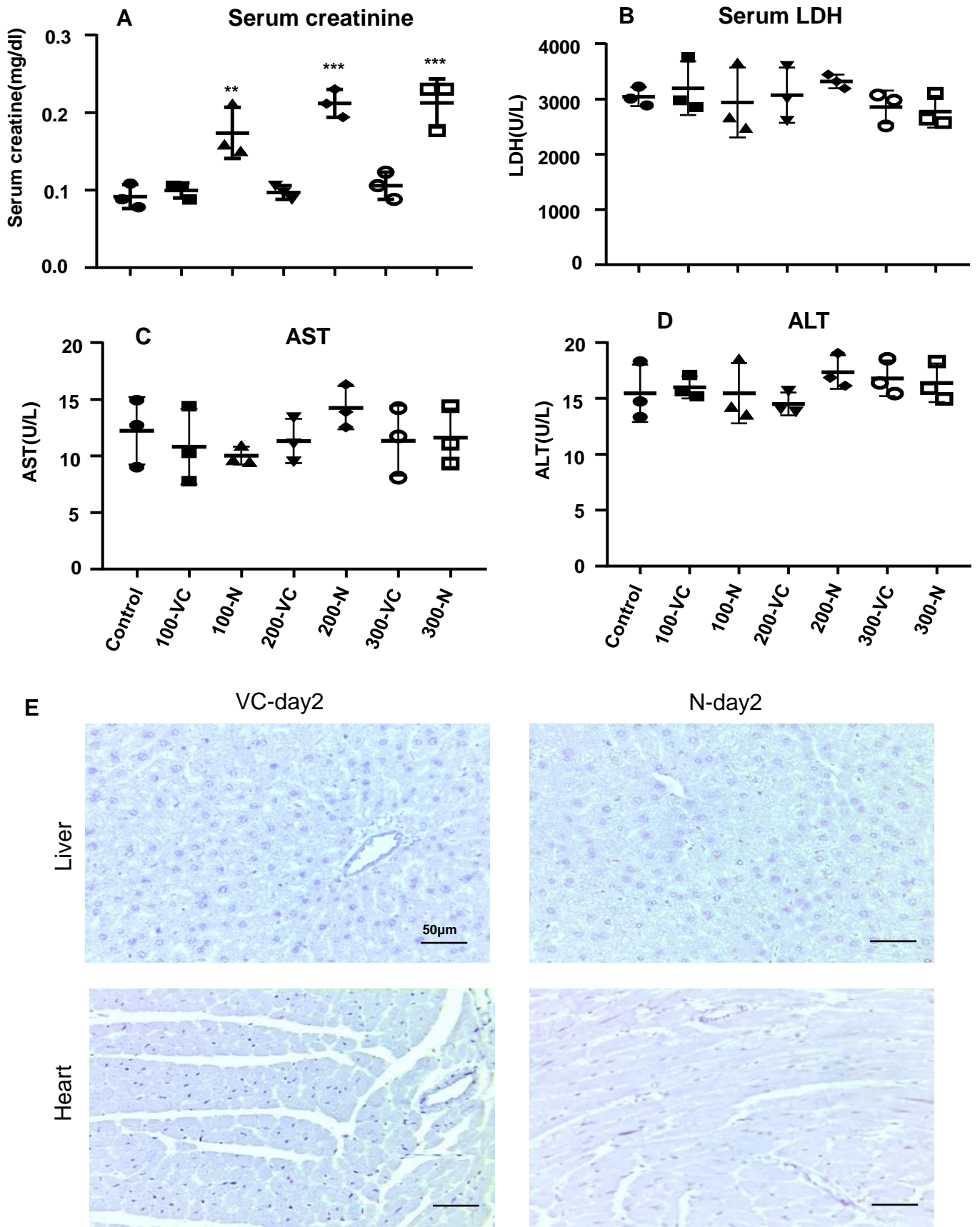


Figure S2. Ultrasound-microbubble-mediated kidney-specifically SARS-CoV-2 N protein (N) expression results in a significant increase in serum creatine in a dose-dependent manner without systemic toxicity. (A) Serum creatinine; (B) serum LDH; (C) AST; (D) ALT; (E) immunohistochemical staining shows that expression of SARS-CoV-2 N protein is not detectable in both liver and heart tissues after ultrasound-microbubble-mediated kidney-specifically SARS-CoV-2 N transfection. Each dot represents one mouse and data are expressed as the mean \pm SEM for groups of 3 mice. ** $p < 0.01$, * $p < 0.001$ versus vector control (VC).**

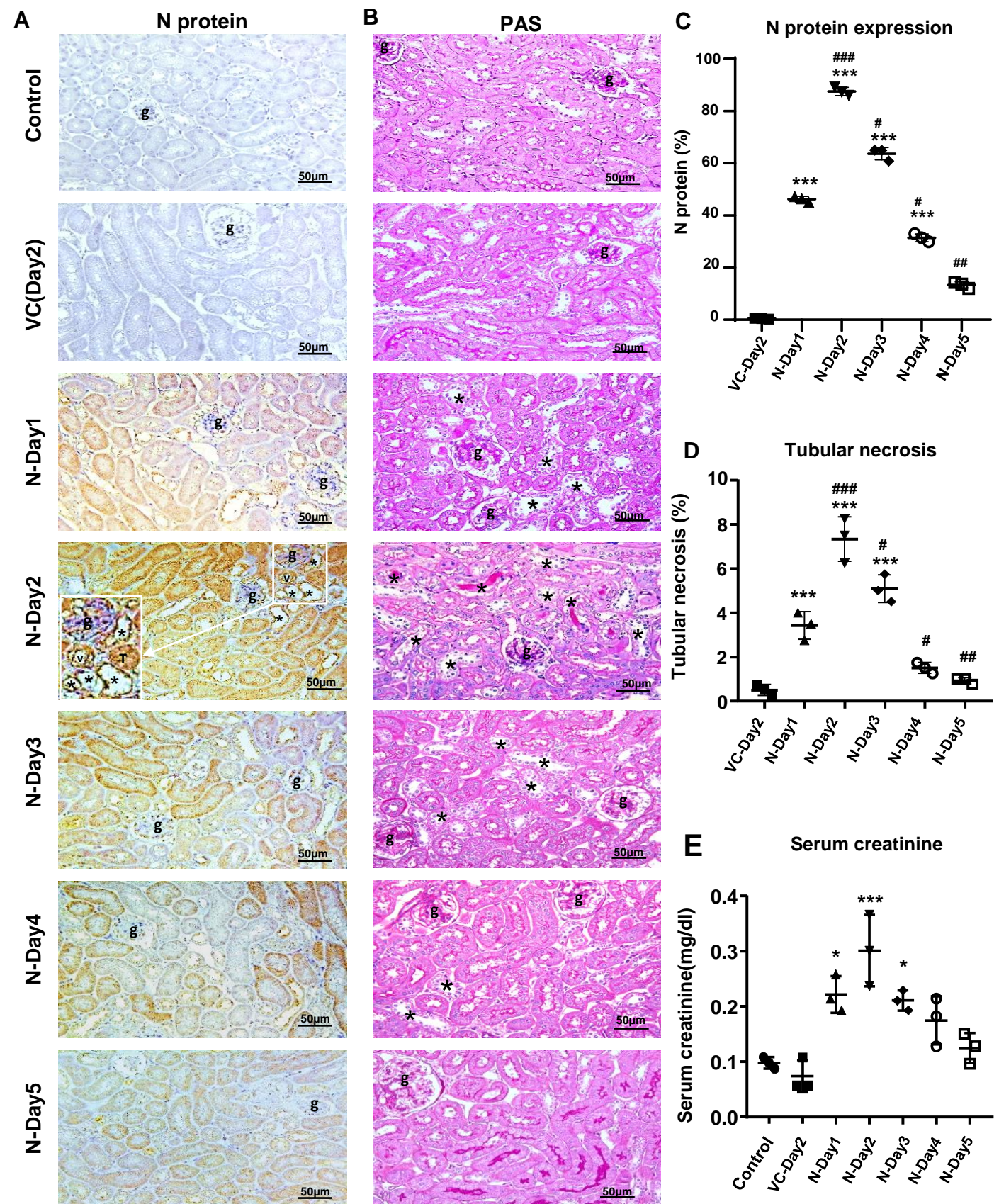


Figure S3. Kidney-specifically overexpressing SARS-CoV-2 N protein (N) causes AKI in a time-dependent manner, peaking at day 2 after the N gene transfer. (A) N protein immunostaining; (B) PAS-staining; (C) Semi-quantitative analysis of N protein; (D) Semi-quantitative analysis of tubular necrosis (*); (E) Serum levels of creatinine. Note that kidney-specifically SARS-CoV-2 N-expressing plasmid transfer results in overexpression of N protein primarily in tubular cells with tubular necrosis (*) as well as in glomerular (g) and vascular (v) cells (see inserted picture at day 2) in a time-dependent manner, peaking at day 2. Each dot represents one mouse and data are expressed as the mean ± SEM for groups of 3 mice. *p<0.05, *p<0.001 versus vector control (VC); #p<0.05, ##p<0.01, ###p<0.001 versus SARS-CoV-2 N-expressing plasmid at day 1 (N-day 1). g, glomerulus. Scale bar=50 μm.**

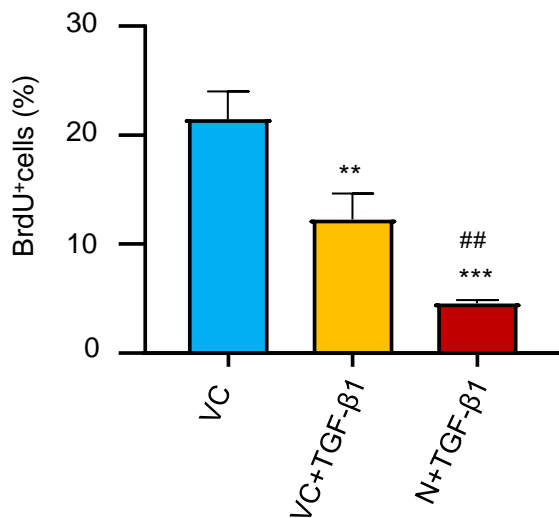
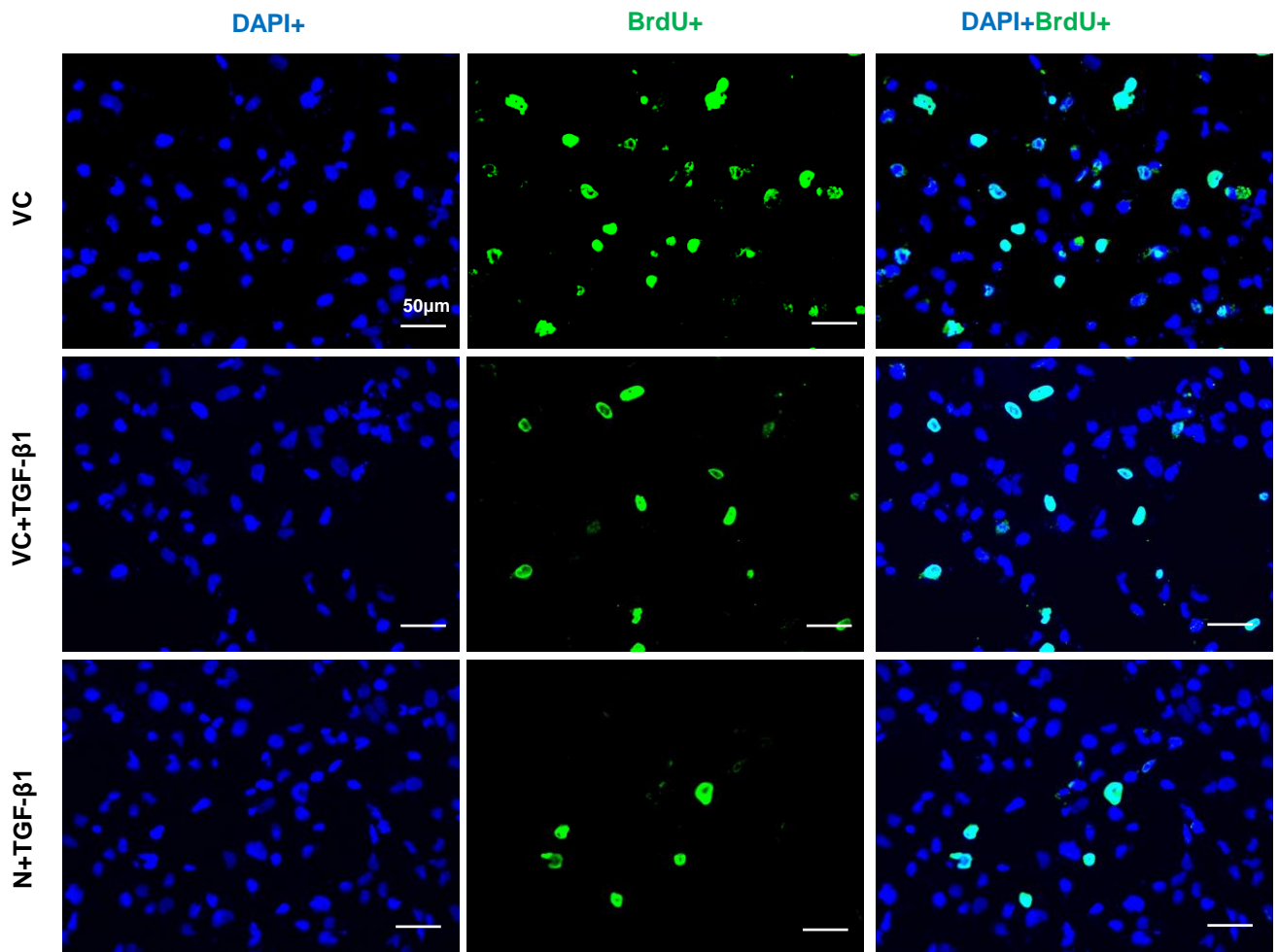


Figure S4. Immunofluorescence detects that overexpressing SARS-CoV-2 N protein (N) largely promotes TGF-β1-induced inhibition of S-phase cell cycle in human TECs (HK-2) in vitro. Note that under normal conditions, HK-2 cells are highly proliferative as demonstrated by many cells entering into the S-phase of cell cycle, which is inhibited by addition of TGF-β1 (5ng/ml) and becomes worsen by co-overexpressing SARS-CoV-2 N protein. Each bar represents the mean \pm SEM for 3 independent experiments. ** $p < 0.01$, *** $p < 0.001$ versus vector control (VC); ### $p < 0.001$ versus VC + TGF-β1. Scale bar=50 μ m.

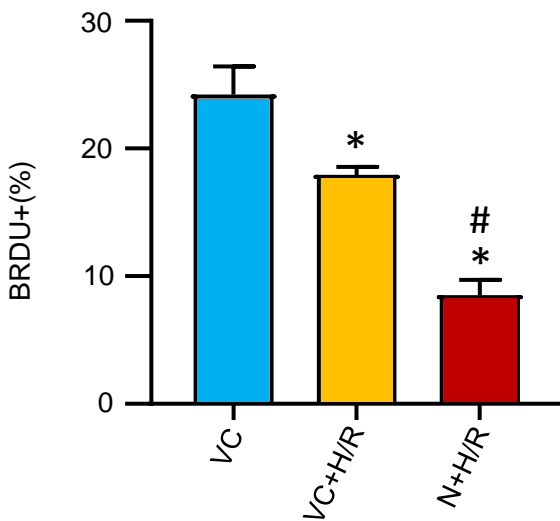
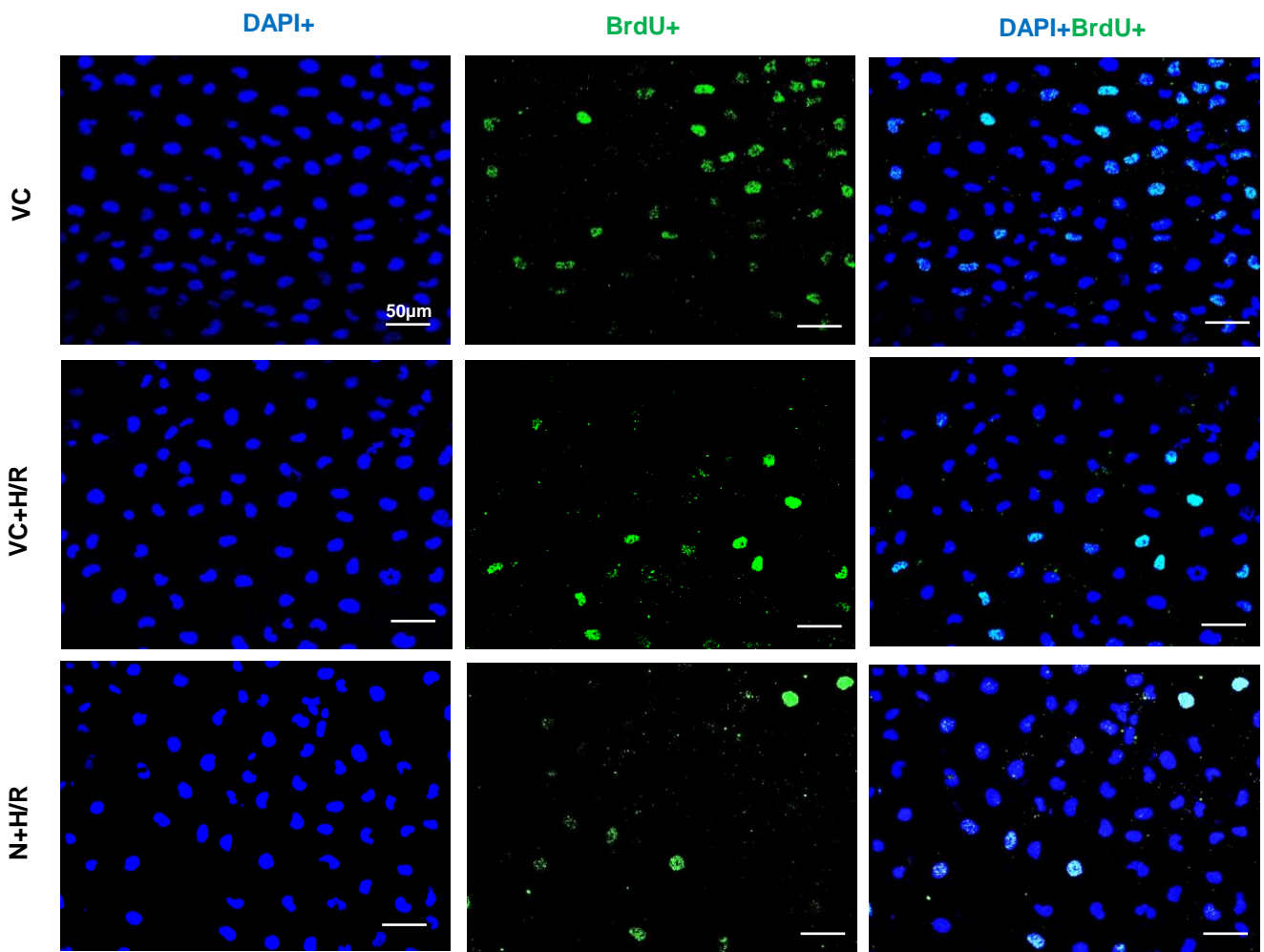


Figure S5. Immunofluorescence detects that overexpressing SARS-CoV-2 N protein (N) largely promotes hypoxia/reoxygenation-induced inhibition of S-phase cell cycle in human TECs (HK-2) in vitro.

Note that under normal conditions, HK-2 cells are highly proliferative as demonstrated by many cells entering into the S-phase of cell cycle, which is inhibited by hypoxia/reoxygenation injury and becomes worsen by overexpressing SARS-CoV-2 N protein. Each bar represents the mean \pm SEM for 3 independent experiments. * $p < 0.05$ versus vector control (VC); # $p < 0.005$ versus VC +H/R. Scale bar=50 μ m.

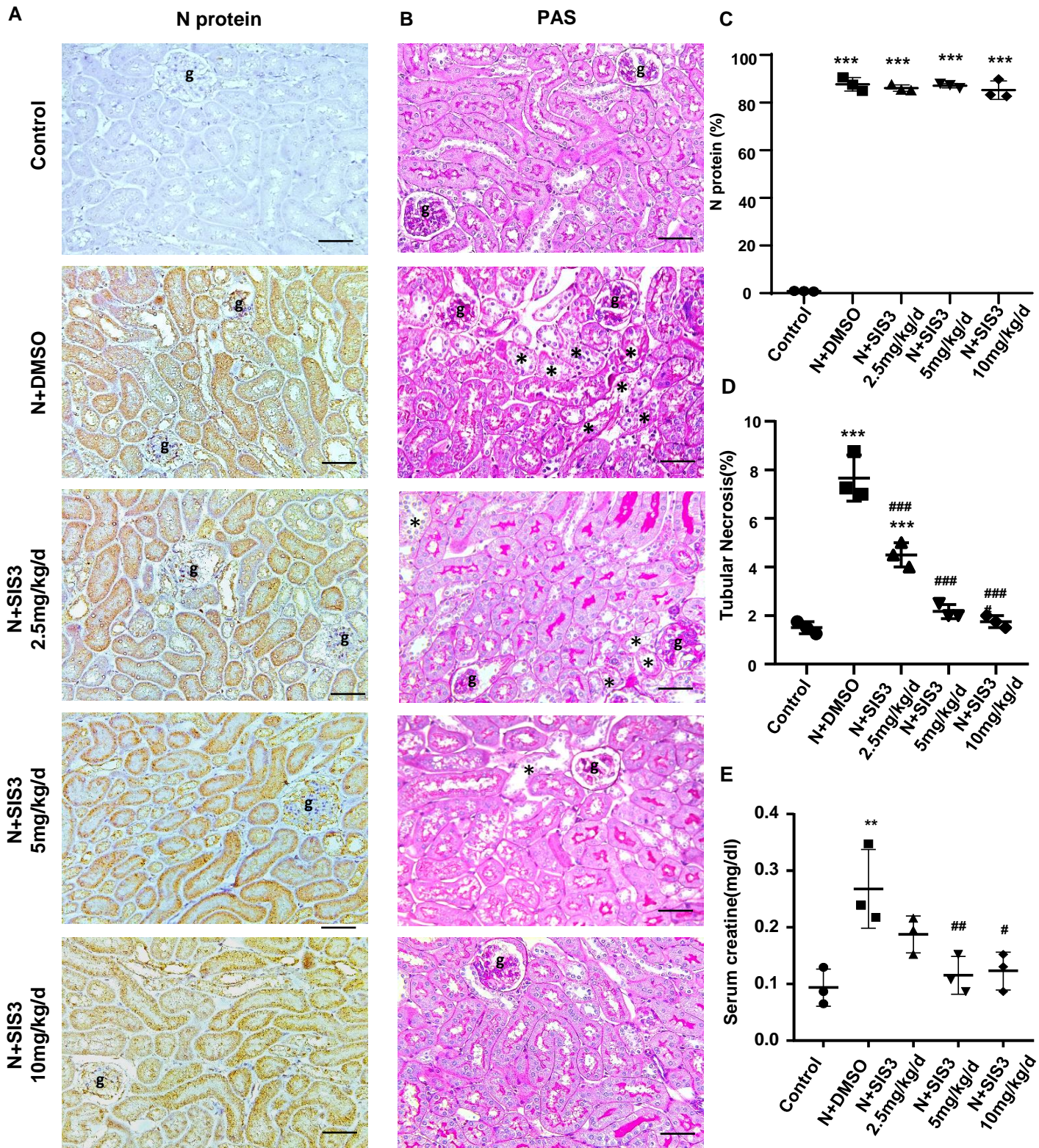


Figure S6. Treatment with SIS3 dose-dependently inhibits SARS-CoV-2 N protein-induced AKI without altering expression of N protein in the kidneys. (A) SARS-CoV-2 N protein immunostaining; **(B)** PAS-staining for detection of tubular necrosis (*); **(C)** Semi-quantitation of the N protein expression in the kidney; **(D)** Semi-quantitation of renal tubular necrosis; **(E)** Serum levels of creatinine. Each dot represents one mouse and data are expressed as the mean \pm SEM for groups of 3 mice. ** $p < 0.01$, *** $p < 0.001$ versus vector control; # $p < 0.05$, ## $p < 0.01$, ### $p < 0.001$ versus overexpression of SARS-CoV-2 N + DMSO-control treatment (N+DMSO). g, glomerulus. Scale bar=50 μ m.

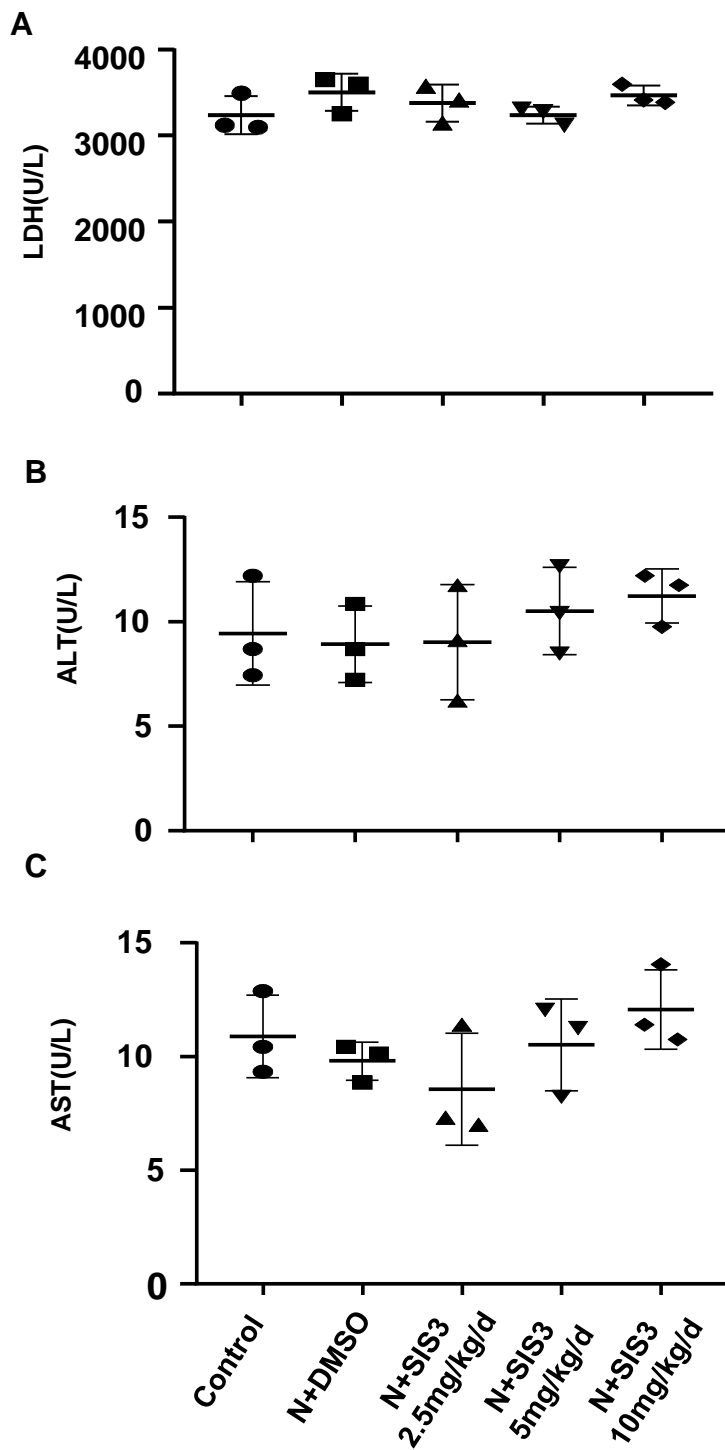


Figure S7. Systemic toxicity of SIS3 in mice with SARS-CoV-2 N protein-induced AKI. (A) Serum levels of LDH release; **(B)** Serum levels of ALT; **(C)** Serum levels of AST. Each dot represents one mouse and data are expressed as the mean \pm SEM for groups of 3 mice.

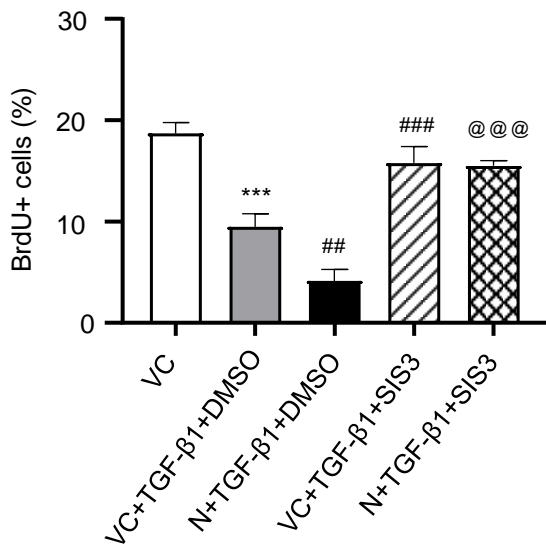
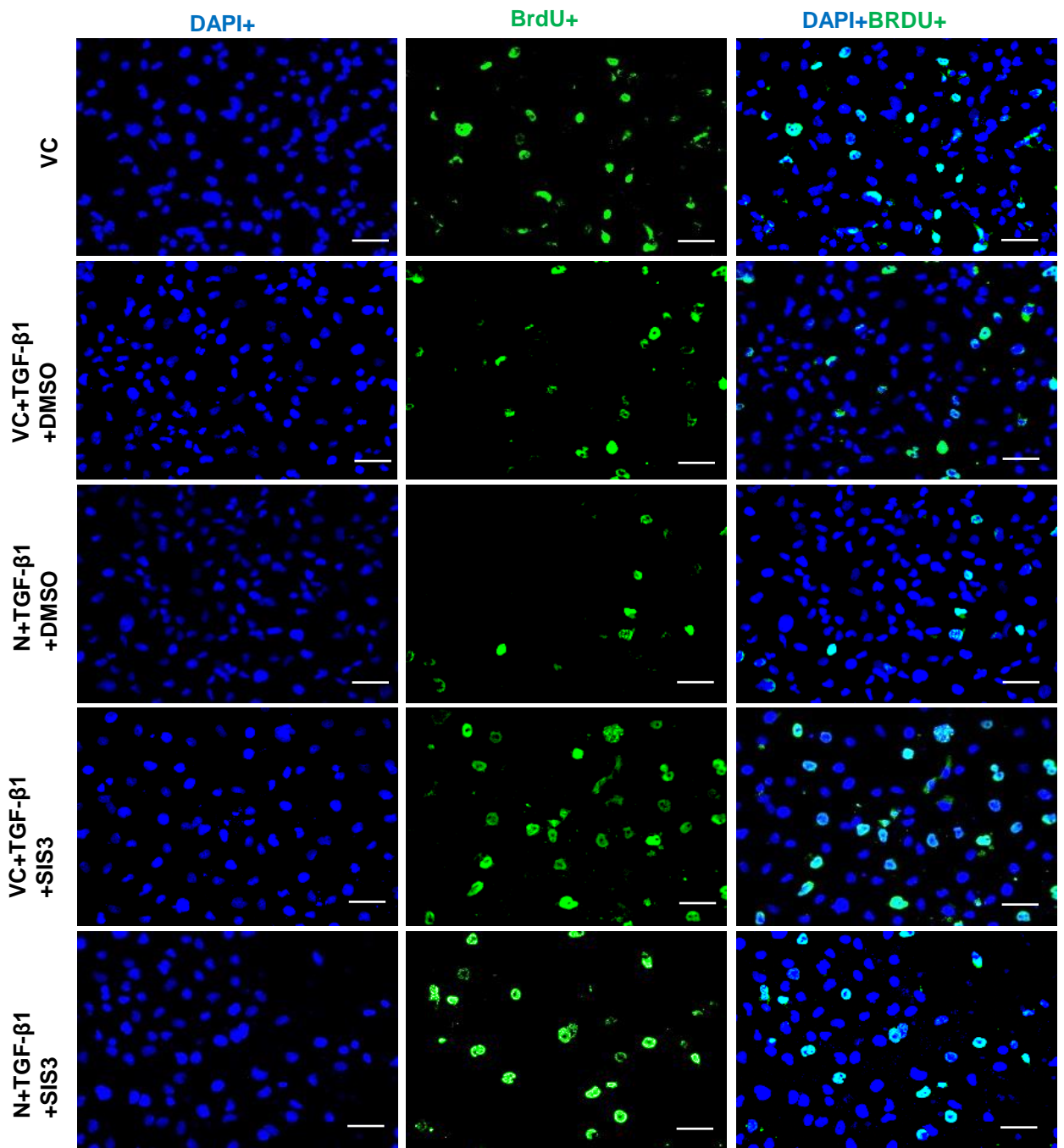


Figure S8. Blockade of Smad3 reverses SARS-CoV-2 N-induced inhibition of cell cycle progression at the S-phase in HK-2 cells in vitro. Immunofluorescence detects that overexpression of SARS-CoV-2 N protein (N) can severely impair TEC proliferation by blocking the S-phase cell cycle progression, which is virtually blocked with a Smad3 inhibitor SIS3. Note that SIS3 treatment also blocks TGF-β1-induced inhibition of S-phase cell cycle in HK-2 cells. Each bar represents the mean \pm SEM for groups of 3 independent experiments. * $p < 0.05$, *** $p < 0.001$ versus vector control (VC); ## $p < 0.01$, ### $p < 0.001$ versus VC+TGF-β1+DMSO; @@@ $p < 0.001$ versus N+TGF-β1+DMSO. Scale bar=50 μ m.